Proceedings of the 9th U.S. National and 10th Canadian Conference on Earthquake Engineering
Compte Rendu de la 9ième Conférence Nationale Américaine et
10ième Conférence Canadienne de Génie Parasismique
July 25-29, 2010, Toronto, Ontario, Canada • Paper No 867

SPECTRAL ACCELERATION ATTENUATION FOR SEISMIC HAZARD ANALYSIS IN IRAN

H. Saffari[1], Y. Kuwata[2], S. Takada[3] and A. Mahdavian[4]

ABSTRACT

Existing attenuation relations in Iran mostly deal with peak ground acceleration and peak ground velocity. However, spectral attenuation is needed not only for peak ground acceleration, but also for the entire range of periods. In this study, a new spectral attenuation for acceleration is presented for Iran. To that end, a database of strong ground motion in Iran consisting of 110 earthquakes and 627 accelerograms was developed. We introduced the attenuation relationship for acceleration response spectra with 5% damping. The two primary factors considered were moment magnitude and source distance. A near field term was also used in the model for better estimation of acceleration spectra in the near field. Non-linear regression analysis adopted from Fukushima and Tanaka (1990) was used to obtain coefficients.

Introduction

For rational seismic design of structures and infrastructures at a site, it is necessary to know the attenuation characteristics of seismic ground motion. Many parameters such as source distance, earthquake magnitude, and geological conditions affect attenuation. Nonetheless, a good model should consider at least the following main variables: earthquake magnitude, shortest distance to the seismic fault plane, and focal depth. In order to improve its predictions, a model may include a regional anomalous seismic intensity correction (Kanno et al. 2006) and local site ground correction (Zhao et al. 2006). To create such a model, it is necessary to compile a large database of strong motion accelerograms and to process them for analysis. Thereafter, a base model that can extract the average characteristics of earthquake ground motion for peak ground acceleration (PGA), peak ground velocity (PGV), or acceleration response spectra should be defined. Period-specific regression analysis of accelerograms yields the corresponding coefficients of the model for that period. Site effects or more factors that indicate local or tectonic conditions can also be applied to the model. Finally, the model should be compared with observed accelerograms in several cases for fit control.

The purpose of this paper is to develop the regression model presented by Fukushima and Tanaka (1990) for Iran's major seismic zones database and to derive the attenuation relationships including the near-source amplification saturation term. An inventory of 110

[1]Ph. D. Student, Dept. of Civil Engineering, Kobe University, Rokkodai 1, Nada, Kobe 657-8501 JAPAN
[2]Associat Professor, Dept. of Civil Engineering, Kobe University, Rokkodai 1, Nada, Kobe 657-8501 JAPAN
[3]Adjunct Professor, Dept. of Civil Engineering, University of Tehran, Keshavarz Blvd, No.268, Tehran, 1417633861, IRAN
[4]Assistant Professor, Dept. of Civil Engineering, Power & Water University of Technology, Tehranpars, Tehran, 16765-1719, IRAN

earthquakes in the Central Iran and Zagros zones consisting of 627 triaxial accelerograms was created. Moment magnitude and the shortest distance to fault plane were selected as the main parameters. A non-linear regression analysis was presented to obtain coefficients by using the model of Fukushima and Tanaka (1990). In this research, site class was divided into two types, rock and soil conditions.

Seismic Activity in Iran

Iran, situated over the Alpine-Himalayan seismotectonic belt, has experienced many strong earthquakes. Earthquakes here are generated in the crustal zone caused by compression between the Eurasian and Arabian plates, which are concentrated in the Alborz mountains on the southern boundary of the Caspian Sea and in the Zagros mountains in the southwest of the country.

Fig. 1 shows seismic zones of Iran drawn by Berberian and Mohajer-Ashjai (1977). This map was obtained from a probabilistic seismic hazard analysis of Iran. Macroseismic information, historical and instrumental seismic data, seismic source, attenuation, and recurrence of earthquakes in all areas of Iran have been studied. Since there are insufficient accelerograms for each zone to be analyzed, researchers usually combine zones into two major zones such as the Central Iran and Zagros zones in their analyses. The two zones are overlaid on Fig. 1. Earthquakes in the Central Iran zone have relatively large magnitude and show the fault fracture on the surface, whereas earthquakes in the Zagros zone are mostly moderate and their fracture plane is not clear. In this study, we investigate the attenuation of earthquakes in the Central Iran and Zagros zones.

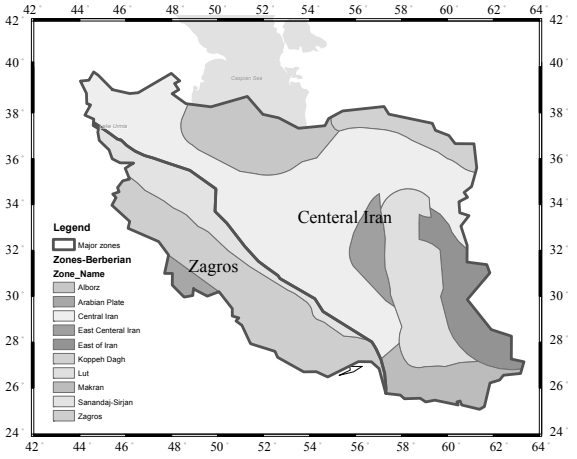

Figure 1. Iran's seismic zones (Berberian and Mohajer-Ashjai, 1977)

Database

In this study, we used 627 accelerograms that were recorded during 110 earthquakes in the Central Iran and Zagros zones. The accelerograms are observed by the Iran Strong Motion Network (ISMN) which is run by the Building and Housing Research Center (BHRC, Iran). Criteria for selection of earthquake events and accelerograms are as follows:

- M_w is not smaller than 5.0,
- Data were recorded on the ground surface (free-field),
- Two orthogonal horizontal components are available,
- Data were truncated at an M_w-dependent source distance.

The moment magnitude and focal depth of the earthquakes were typically taken from the earthquake catalog of Department of Earth and Planetary Sciences and the Division of Engineering and Applied Science at Harvard University. In some special cases, the data were extracted from the BHRC website. The distribution of the database regarding magnitude-source distance and magnitude-focal depth are shown in Figs. 2 and 3, respectively. The source distance ranges from 4 km to around 200 km. The earthquakes with M_w over 6.0 have relatively shallow focal depth, and the others have a depth of 7 to 72 km.

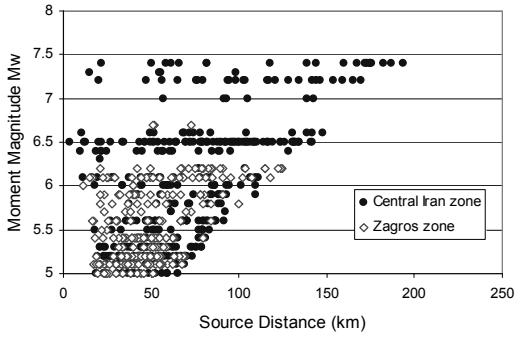

Figure 2. Magnitude-distance distribution

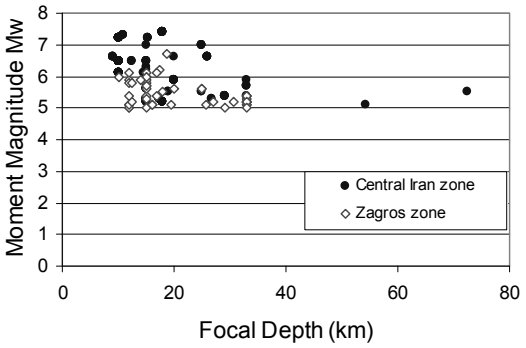

Figure 3. Magnitude-focal depth distribution

Parameter X in this study is the source distance. For earthquakes with magnitudes greater than 6.5, the length of fault rupture was considered in the calculations. For the others, the distance to the hypocenter of the earthquake was considered.

The truncation of data at an M_w-dependent source distance used the following control of response spectra (Fukushima et al. 2000):

$$f(M_w, X) > \log 10 \tag{1}$$

and

$$f(M_w, X) = 0.42M_w - \log(X + 0.025 \times 10^{0.42M_w}) - 0.0033X + 1.22 \tag{2}$$

Subsequently, the data were corrected after the first regression analysis. In this regard, the data were truncated again by the condition in which the right term of Eq. 1 is replaced by $1 + \sigma$ (standard deviation). This change was made because the trigger level of a seismometer cannot record less than 10 gal. This correction balances (shifts down) predicted acceleration curves to the real values as shown by Matsusaki et al. (2006).

As accelerograms recorded by seismometers were not corrected, we used two correction methods, baseline and filtering. A bandpass filter used in this study is ranging from 0.2 to 20 Hertz considering instrument characteristics of SSA2 (digital) and SMA1 (analog) of ISMN. The acceleration spectrum with 5% damping was obtained at 0.05 s intervals from 0.05 to 1.0 s, 0.2 s intervals from 1.0 to 3.0 s, and then 0.5 s intervals from 3.0 to 5.0 s.

Finally, data distributions were examined for each magnitude with respect to amplitude and source distance, and those events having irregular distributions (by particular geological tectonic or other effects) were eliminated.

Regression Model

The seismic ground motion at a site can generally be explained by source parameters, wave propagation, and site amplification. Eq. 3 shows this relationship as it depends on frequency (f):

$$A_{ij}(f) = S_i(f) \cdot P(f) \cdot G_j(f) \tag{3}$$

,where $A_{ij}(f)$ is the seismic ground motion of earthquake i at site j, $S_i(f)$ is the source characteristics of earthquake i, $P(f)$ is the propagation characteristics, and $G_j(f)$ is the local site amplification characteristics at site j. Propagation characteristics can be shown in terms

of a Green's function:

$$P(f) = \frac{1}{X} \exp\left(\frac{-\pi f X}{Q\beta}\right) \tag{4}$$

In the former equation, X is the source distance, Q is the quality factor, and β is the shear wave velocity in the crustal zone. The first term on the right is a geometric attenuation term, and the second term is an inertial attenuation term. By replacing $P(f)$ with Eq. 4 and taking the logarithm of both sides of the equation, the following relation will be obtained:

$$\log A_{ij}(f) = a(f) \cdot M_w - \log X - b(f) \cdot X + g_J(f) \tag{5}$$

To improve the near-source predictive ability of the model, parameter $d \cdot 10^{e(f) \cdot M_w}$ is added to the second term of X in order to weight the data in small amounts of X (near source). The model can be developed by period instead of frequency. We considered two coefficients c_R and c_S for rock and soil as geological conditions in the following:

$$\log A_{ij}(T) = a(T) \cdot M_w - \log(X + d(T) \cdot 10^{e(T) \cdot M_w}) - b(T) \cdot X + \sum c_i(T) L_i \tag{6}$$

In the above model M_w is moment magnitude, X is the closest distance from the site to the fault plane, and a, b, c, d and e are coefficients of regression analysis. Parameters c_R and c_S for coefficient c_i are rock and soil coefficients, respectively. If the site is rock, L_R is 1 and L_S is 0, otherwise (if the site is soil) L_R is 0 and L_S is 1.

Method of Analysis

In this study, a two-step regression analysis introduced by Fukushima and Tanaka (1990) was applied to the database of Iran's major zones. First, the distance coefficients such as $b(T)$ and $d(T)$ were obtained using dummy variables for individual events. Parameters $a(T)$, $c_R(T)$, and $c_S(T)$ were determined using the $b(T)$ and $d(T)$ coefficients derived in the first step.

As the $d(T)$ and $e(T)$ coefficients are a bias relation, the $e(T)$ coefficient was fixed at 0.5, as suggested from previous studies. To obtain $d(T)$, since the model is non-linear in the regression analysis, a nonlinear solution like Newton's method may be used. The differences between the predicted and observed values can be written as,

$$\varepsilon_i = \log Sa_i(T) - \{a(T)M_i - \log(X_i + d(T) \cdot 10^{e(T)M_i}) - b(T) \cdot X_i + \sum c_i(T) L_i\} \tag{7}$$

where $Sa_i(T)$ is observed acceleration spectra of datum i, and i indicates individual data points.

In our method, regression analysis was performed for the rock data and parameters $a(T)$, $b(T)$, $c_R(T)$, and $d(T)$ were determined. For soil data we used the same $a(T)$, $b(T)$, and $d(T)$ coefficients derived from the rock data, and then we obtained $c_S(T)$ by a simple calculation.

In order to make the attenuation coefficients useful in the future, the coefficients were smoothed based on a polynomial equation (Kinoshita et al., 1986) as follows:

$$Y(T) = Y_0 + \sum_{i=1}^{m} Y_i \cdot (\log T)^i \tag{8}$$

where $Y(T)$ is the coefficient in the attenuation model, Y_0 and Y_i are regression coefficients for the smoothed curve and T is period. In this study, m was considered 5.

Results

The results of the regression analysis for Central Iran and Zagros zones are shown in Fig. 4. These period curves were obtained and drawn up to 5 s. Fig. 4(a) shows the coefficient of moment magnitude which increases as the period increases. The coefficient of distance (b) has a higher rate of decrease in short period for Zagros zone than Central Iran zone, it then decreases at a lower rate in the long period. The coefficients of site conditions are shown in Fig. 4(c) and (d) for Central Iran and Zagros zones respectively. Values for c_S are a little more than c_R due to amplification of soil layers. The standard errors are stable, ranging from 0.29 to 0.4 for rock and soil data. Table 1 summarizes the coefficients of spectral attenuation related to Central Iran and Zagros zones. The coefficient of distance saturation, d(T), is small and provides minimum error in trials among the numbers over 0.005 for all periods in the regression analysis. As the result of this study, the coefficient of distance saturation, d(T), in all periods was found to be 0.005.

Predicted acceleration response spectra for Central Iran and Zagros zone are shown in Figs. 5 and 6 in two ranges of ground at the site and three ranges of distance for some cases of magnitude. The maximum acceleration in the rock for the Central Iran zone at the distance of 20 km is 370 gal at 0.15 sec for M_w 6.0 and 800 gal at 0.15 sec for M_w 7.0. As for the Zagros zone, the ranges of the database do not cover near source, far distance, and large magnitudes. Thus, the prediction was performed only for 40 and 60 km and moment magnitudes of 5.5 and 6.0. The spectra of rock have a peak that is 1.5 times higher than those of soil at 0.15 s at the near source site. The difference of peaks between rock and soil becomes less relevant when the source distance becomes far. In contrast, the spectra of soil are larger than those of rock over 0.4 s due to ground amplification. Since the classification of the ground type is very severe for rock data, the predicted spectra exhibit such a strong peak.

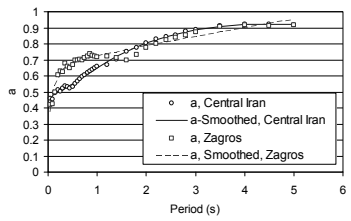

(a) Coefficient of magnitude

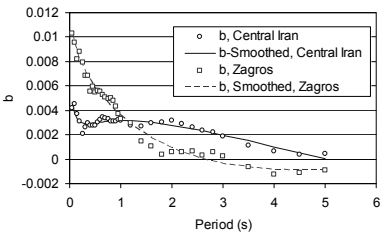

(b) Coefficient of distance

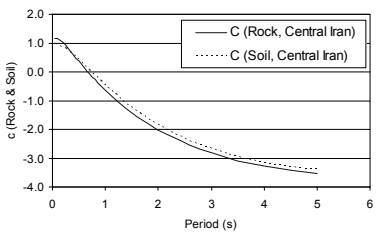

(c) Coefficient of site in Central Iran Zone

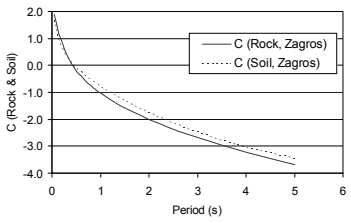

(d) Coefficient of site in Zagros Zone

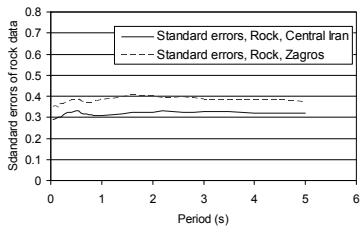

(e) Standard error for rock data

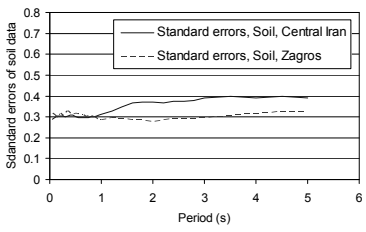

(f) Standard error for soil data

Figure 4. Coefficients of regression analysis for Central Iran and Zagros zones

Table 1. Coefficients of regression analysis for Central Iran and Zagros zones

(a) Coefficients for Central Iran zone

Period	a	b	c_{Rock}	c_{Soil}	σ_{Rock}	σ_{Soil}
0.05	0.450	0.0047	1.158	0.992	0.291	0.289
0.1	0.478	0.0038	1.154	0.934	0.293	0.295
0.15	0.490	0.0033	1.094	0.899	0.300	0.303
0.2	0.498	0.0031	1.011	0.860	0.301	0.303
0.25	0.505	0.0029	0.914	0.809	0.312	0.304
0.3	0.512	0.0029	0.809	0.746	0.320	0.302
0.4	0.530	0.0029	0.588	0.595	0.325	0.308
0.5	0.549	0.0030	0.365	0.425	0.330	0.301
0.6	0.570	0.0030	0.146	0.245	0.320	0.297
0.7	0.590	0.0031	-0.065	0.063	0.316	0.296
0.8	0.611	0.0031	-0.267	-0.118	0.312	0.300
0.9	0.631	0.0031	-0.459	-0.295	0.307	0.305
1	0.651	0.0032	-0.641	-0.467	0.310	0.313
1.5	0.736	0.0031	-1.416	-1.228	0.320	0.358
2	0.803	0.0028	-2.015	-1.840	0.322	0.372
2.5	0.851	0.0024	-2.470	-2.313	0.326	0.375
3	0.886	0.0020	-2.823	-2.680	0.326	0.388
4	0.920	0.0010	-3.287	-3.158	0.322	0.390
5	0.920	0.00002	-3.525	-3.382	0.319	0.390

(b) Coefficients for Zagros zone

Period	a	b	c_{Rock}	c_{Soil}	σ_{Rock}	σ_{Soil}
0.05	0.376	0.0103	1.892	1.690	0.351	0.316
0.1	0.473	0.0095	1.543	1.239	0.356	0.306
0.15	0.540	0.0087	1.168	0.890	0.346	0.297
0.2	0.582	0.0081	0.864	0.646	0.365	0.315
0.25	0.611	0.0076	0.617	0.463	0.366	0.303
0.3	0.632	0.0072	0.411	0.317	0.368	0.315
0.4	0.659	0.0065	0.079	0.086	0.382	0.317
0.5	0.676	0.0058	-0.182	-0.099	0.382	0.315
0.6	0.689	0.0053	-0.399	-0.259	0.377	0.311
0.7	0.699	0.0048	-0.585	-0.404	0.369	0.302
0.8	0.707	0.0043	-0.749	-0.538	0.370	0.304
0.9	0.715	0.0039	-0.897	-0.665	0.377	0.293
1	0.722	0.0035	-1.031	-0.785	0.387	0.286
1.5	0.755	0.0020	-1.576	-1.315	0.401	0.289
2	0.786	0.0009	-2.004	-1.764	0.398	0.278
2.5	0.816	0.0002	-2.362	-2.149	0.394	0.292
3	0.845	-0.0003	-2.677	-2.485	0.384	0.295
4	0.900	-0.0009	-3.217	-3.034	0.381	0.317
5	0.949	-0.0009	-3.677	-3.458	0.374	0.324

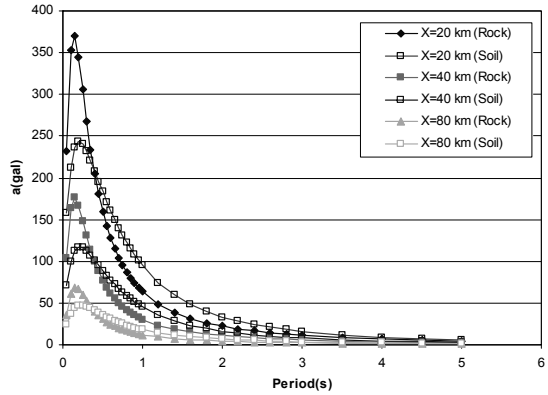

(a) $M_w = 6.0$

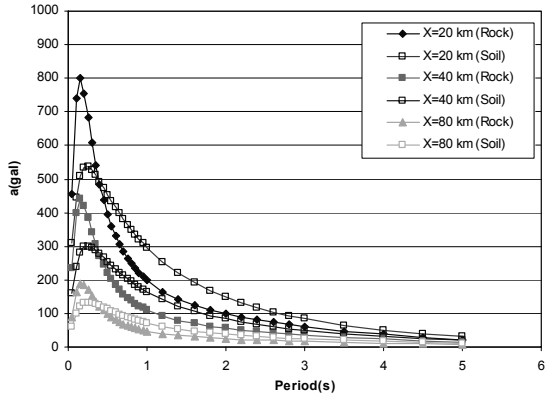

(b) $M_w = 7.0$

Figure 5. Estimated acceleration response spectra for the Central Iran zone (20, 40 and 80 km)

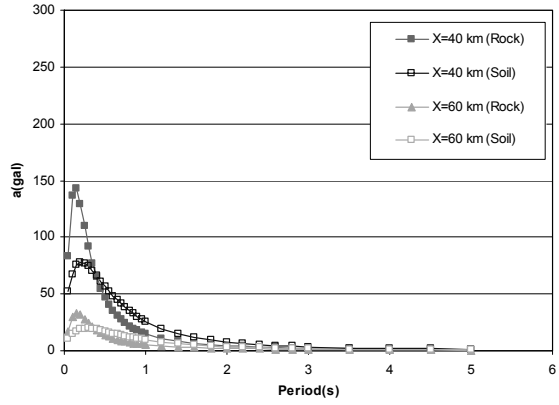

(a) $M_w = 5.5$

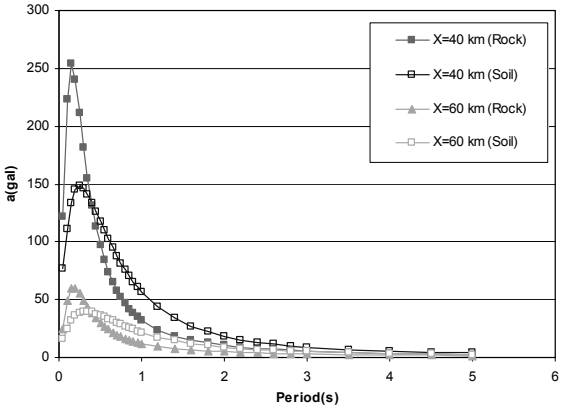

(b) $M_w = 6.0$

Figure 6. Estimated acceleration response spectra for the Zagros zone (40 and 60 km)

Comparison with Previous Research in Iran and Japan

For better understanding, predicted acceleration spectra in the present study and from other research in Japan and Iran were compared for moment magnitudes 6.0 and 7.0 and distances of 20, 40 and 80 km (Figs. 7 and 8). The researchers selected in this comparison were Annaka et al. (1997), Kanno et al. (2006), Uchiyama and Midorikawa (2006), Zhao et al. (2006), Kataoka et al. (2006), and Ghasemi et al. (2008). The first five studies examined attenuation with accelerograms from Japan, whereas the last study by Ghasemi used data from Iran and some data from West-Eurasia and the Kobe earthquake accelerograms of Japan. Some research also showed deep earthquakes, but the comparison was performed for crustal earthquakes.

Results show that in the short periods between 0.05 to 0.3 s, the predicted acceleration spectra for Iran from the present study are a little more than the average value for Japan. This difference can be explained by tectonics of the desired area of study (Iran versus Japan). Another reason is the usage of shortest distance to the fault plane. It should be mentioned that the calculation of short distance was conducted for earthquakes having a rupture on the surface. For large earthquakes that are ruptured on the surface, the distance was calculated to the fault rupture. In contrast, for moderate earthquakes, there was not any fault rupture on the surface, so the distance to the hypocenter was used. Using corrected distances (from site to fault plane) leads to lower predicted acceleration in the near source. For periods more than 0.3 s, the predicted acceleration spectra in this study show a good fit with the average of predicted accelerations of Japanese research. As can be seen in Figs. 7 and 8, the acceleration spectra in the near source show a strong peak.

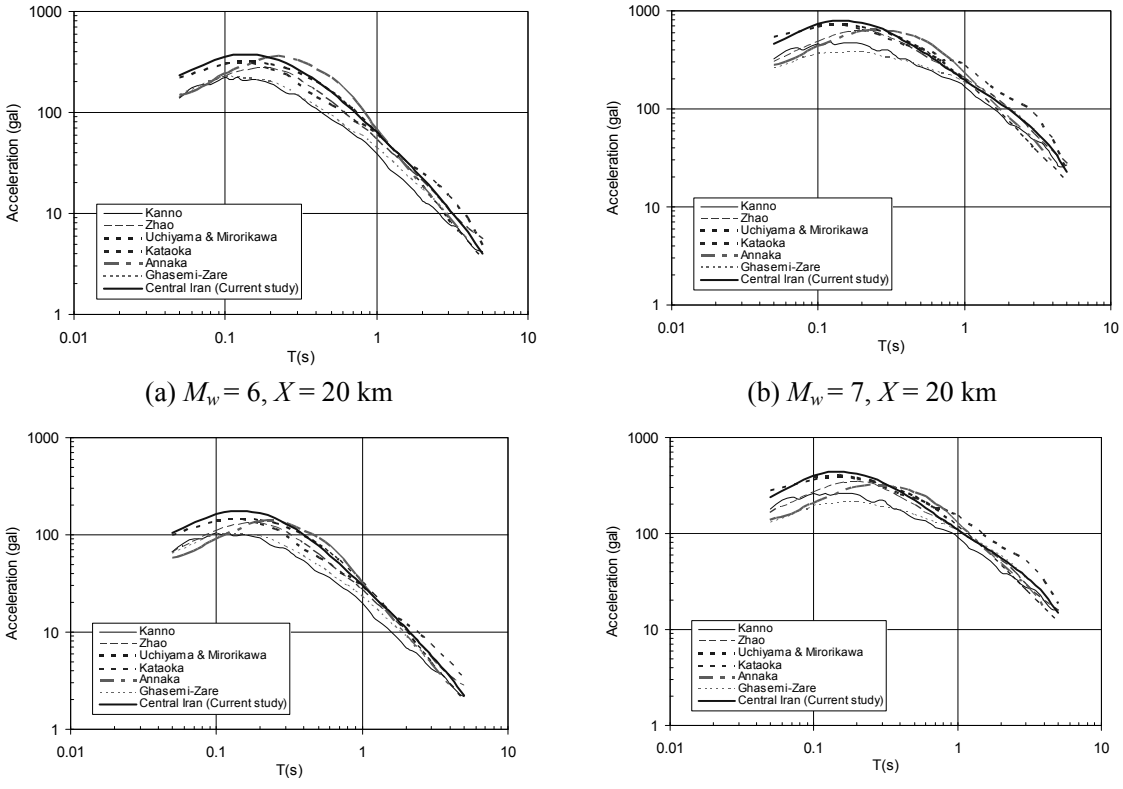

(a) $M_w = 6$, $X = 20$ km

(b) $M_w = 7$, $X = 20$ km

(c) $M_w = 6$, $X = 40$ km

(d) $M_w = 7$, $X = 40$ km

Figure 7. Comparison for predicted acceleration of Central Iran zone for magnitudes of 6.0 and 7.0 at distances of 20, 40 and 80 km

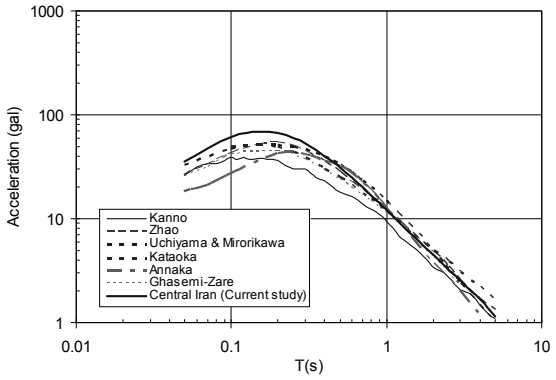

(e) $M_w = 6$, $X = 80$ km

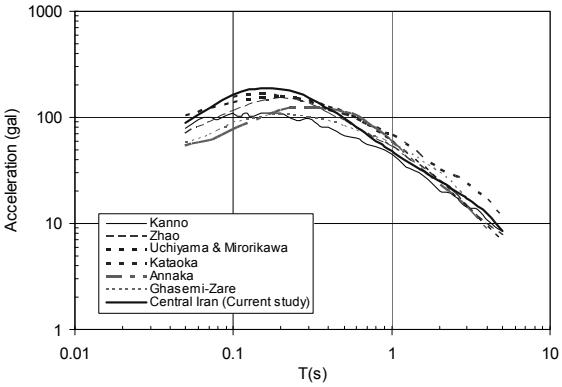

(f) $M_w = 7$, $X = 80$ km

Figure 7. Comparison for predicted acceleration of Central Iran zone for magnitudes of 6.0 and 7.0 at distances of 20, 40 and 80 km (cont.)

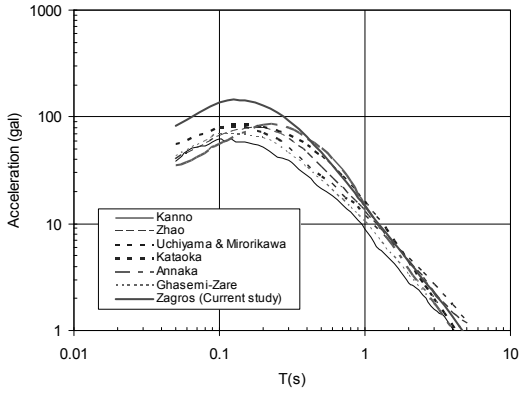

(a) $M_w = 5.5$, $X = 40$ km

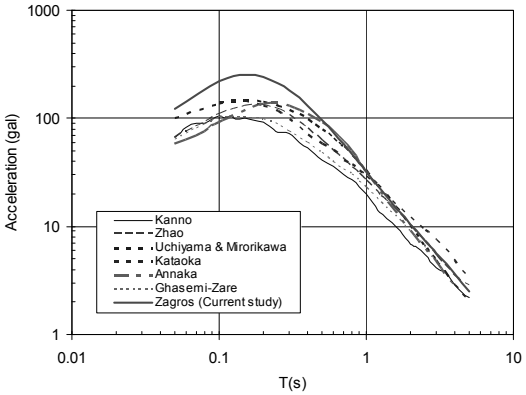

(b) $M_w = 6.0$, $X = 40$ km

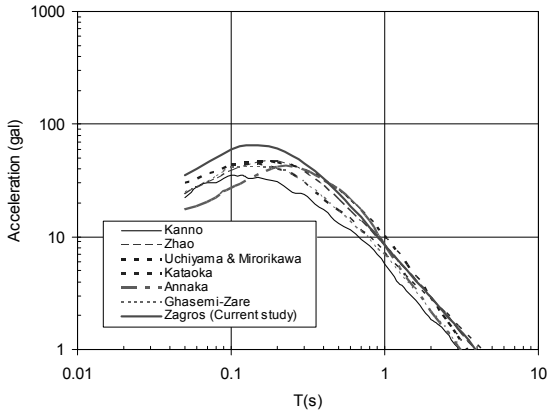

(c) $M_w = 5.5$, $X = 60$ km

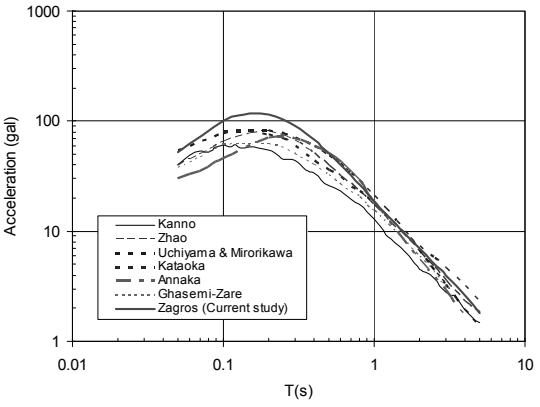

(d) $M_w = 6.0$, $X = 60$ km

Figure 8. Comparison for predicted acceleration of Zagros zone for magnitudes of 5.5 and 6.0 at distances of 40 and 60 km

In future, it will be necessary to examine the ground condition of the site in detail and its effects on these predicted spectra. There is a difference between predicted acceleration in this study from previous research for Iran conducted by Ghasemi et al. (2008). The attenuation model, data handling, and regression method may cause this difference. The

following reasons can be considered:

1-Accelerograms used in this study are not only limited in distance, but are also limited to less than 100 km.

2-Accelerograms in the present study consist of 627 records from the Central Iran and Zagros zones, whereas Ghasemi et al.'s database involves 716 triaxial accelerograms of Iran plus 177 accelerograms from West-Eurasia and data recorded due to the Kobe earthquake in Japan.

Conclusions

In this study, a database consisting of 110 earthquakes and 627 triaxial accelerograms was gathered for the Central Iran and Zagros zones. Regression analysis including the near source term was conducted to estimate spectral attenuation. The method of analysis used in this study can be summarized as follows:

- Two-step regression analysis was used to avoid interaction between the coefficients of moment magnitude and source distance.
- Weighting data for the near source was used to improve the predicted response.
- Since the observed accelerograms have the limitation of trigger lever, the data extraction used the magnitude and distance relation under the condition of the trigger level plus deviation.
- Site classes were considered in the model as two coefficents for rock and soil.

The results of this study can be summarized as follows:

- The standard errors of the rock and soil attenuation models were stable and showed better results for the two-step regression curve.
- The spectra of rock have a peak that is 1.5 times higher than those of soil at T=0.15 s at the near source site. The difference of peak height between rock and soil is less relevant when the source distance becomes far. In contrast, the spectra of soil are larger than those of rock over 0.4 s due to ground amplification.
- Comparison of spectral acceleration with research in Japan shows that the present model has a little more acceleration in case of short periods less than 0.3 s. This difference may emerge from the database or tectonics of the desired area of study. Nevertheless, there is a good fit between predicted acceleration in the present study and the average of the research in Japan, which predicted acceleration in periods more than 0.3 s.

References

Annaka, T., F. Yamazaki, and F. Katahira, 1997. A proposal of an attenuation model for peak ground motions and 5% damped acceleration response spectra based on the JMA-87 type strong motion accelerograms, in Proc. *24th JSCE Earthquake Eng. Symposium*, 161–164 (in Japanese).

Berberian, M., and A., Mohajer-Ashjai, 1977. Seismic risk map of Iran, a proposal, *Geol. Surv. Iran*, 41, 121–148.

Department of Earth and Planetary Sciences and the Division of Engineering and Applied Science at Harvard University, Harvard seismology, *http://www.seismology.harvard.edu* (access 2009. Oct)

Fukushima, Y. and T. Tanaka, 1990. A new attenuation relation for peak horizontal acceleration of strong earthquake ground motion in Japan, *Bull. Seism. Soc. Am.* 80, 757–783.

Fukushima, Y., Irikura, K., Uetake, T., and H. Matsumoto, 2000. Characteristics of observed peak amplitude for strong ground motion from the 1995 Hyogo-ken Nanbu (Kobe) earthquake, *Bull. Seism. Soc*. *Am.* 90, 545–565.

Ghasemi, H., M. Zare, Y. Fukushima, and K. Koketsu, 2008. An empirical spectral ground-motion model for Iran, *Journal of Seismology*, 13, 499–515.

Kanno, T., A. Narita, N. Morikawa, H. Fujiwara, and Y. Fukushima, 2006. A new attenuation relation for strong ground motion in Japan based on recorded data, *Bull. Seism. Soc*. *Am.*, 96(3), 879–897.

Kataoka, S., T. Satoh, S. Matsumoto, and T. Kusakabe, 2006. Attenuation relationships of ground motion intensity using short period level as a variable, *Journal of Structural Mechanics and Earthquake Engineering, JSCE*. A. 62(4), 740–757.

Kinoshita, S., T. Mikoshiba and T. Hoshino, 1986. Average amplification characteristic of S wave in short period in accumulative layer, *Journal of the Seismological Society of Japan*, 39(1), 67-80 (in Japanese).

Matsusaki, S., Hisada, Y., and Y. Fukushima, 2006. Attenuation relation of JMA seismic intensity applicable to near source region*, J. Struct. Constr. Eng.*, AIJ, No. 604, 201–208 (in Japanese).

Uchiyama, Y. and S. Midorikawa, 2006. Attenuation relationship for response spectra on engineering bedrock considering effects of focal depth, *J. Struct. Constr. Eng.*, AIJ, No. 606, 81–88 (in Japanese).

Zhao, J. X., J. Zhang, A. Asano, Y. Ohno, T. Oouchi, T. Takahashi*,* H. Ogawa, K. Irikura, H. K. Thio, P. G. Somerville, Y. (Yasuhiro) Fukushima, and Y. (Yoshimitsu) Fukushima, 2006. Attenuation relations of strong ground motion in Japan using site classification based on predominant period, *Bull. Seism. Soc*. *Am.*, 96(3), 898–913.